



Sandia
National
Laboratories

Detailed evaporation modelling for gasoline direct injection: iso- octane vs. E30

Marco Arienti and Everett Wenzel

ILASS-Americas 32nd Annual Conference on Liquid Atomization and Spray Systems

May 22-25, 2022

Sponsor: U.S. DOE Office of Vehicle Technologies

Program Managers: Gurpreet Singh, Michael Weismiller

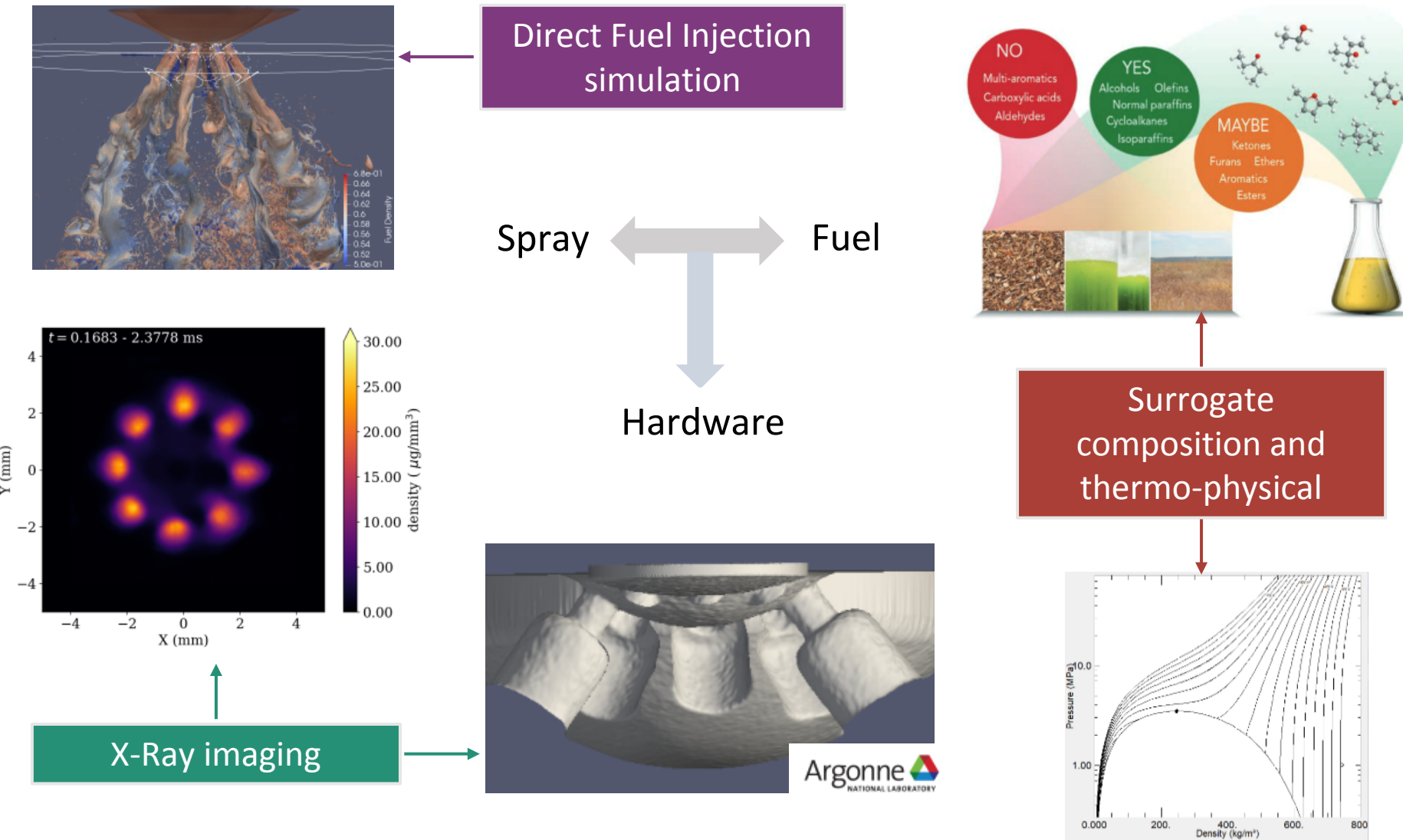


Co-Optimization
of
Fuels & Engines



Sandia National Laboratories is a multimission laboratory managed and operated by National Technology & Engineering Solutions of Sandia, LLC, a wholly owned subsidiary of Honeywell International Inc., for the U.S. Department of Energy's National Nuclear Security Administration under contract DE-NA0003525.

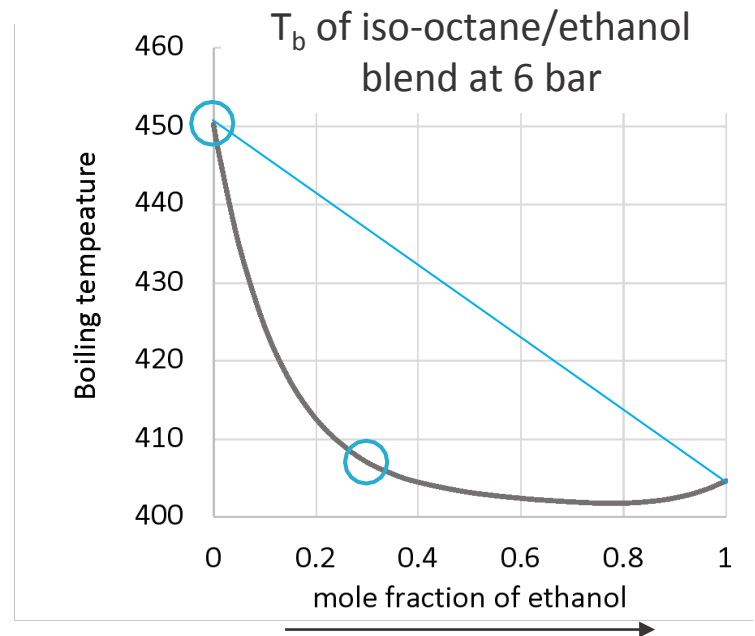
Co-Optima approach



Co-Optima challenges

- Gasoline/ethanol blends do not behave like an ideal mixture (alcohol is a polar substance and iso-octane is non-polar):
 - Non-linear effects (azeotrope)

- Do individual species need to be individually tracked?
 - Infinitely fast (infinite-conductivity model) vs. finite thermal and mass diffusion



$$Pe_l = \frac{K_s}{D_l} = \frac{\text{surface regression rate}}{\text{liquid interdiffusion rate}}$$

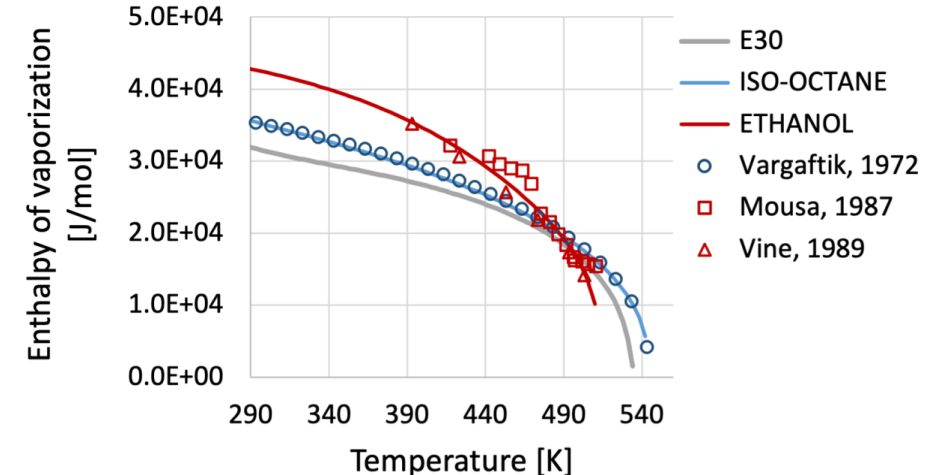
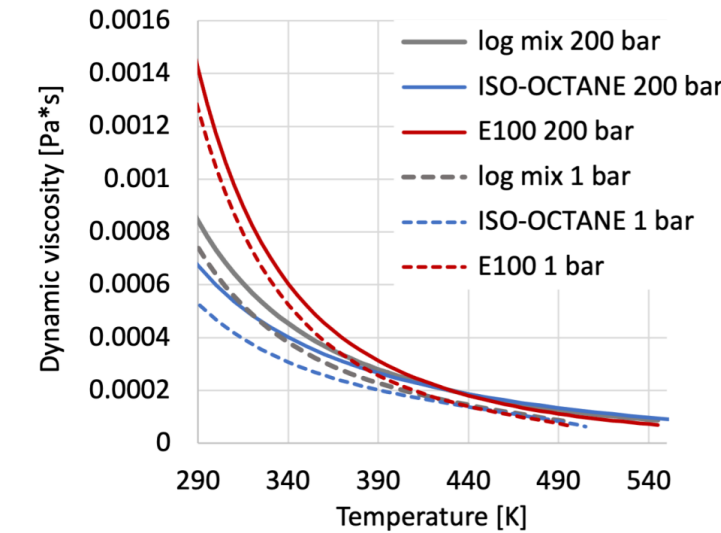
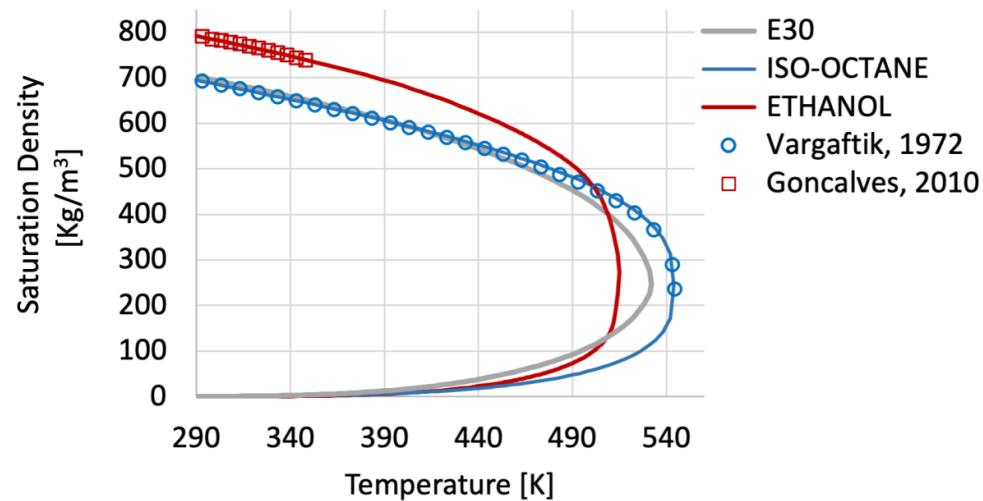
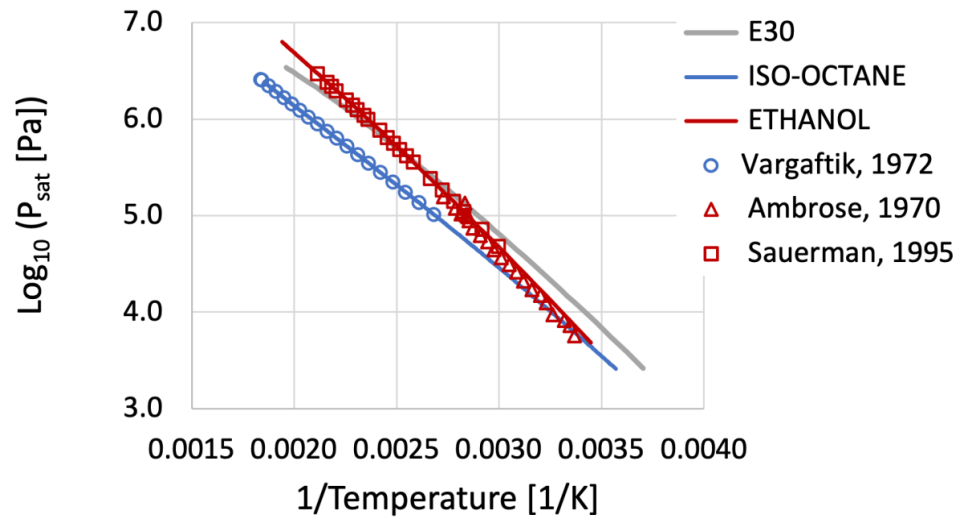
$$\text{(for spherical symmetry: } Pe_l = \frac{\dot{m}_v}{4\pi R D_l \rho_l} \text{)}$$

- There are two limit cases:

$Pe \ll 1$: distillation

$Pe \gg 1$: co-evaporation

Mixing rules based on the Helmholtz energy of the components with departure function for E30



Computational approach: the interface-capturing code CLSVOF



In collaboration with FSU and the LBNL AMReX co-design center

- Sharp-interface discretization of multi-phase Navier-Stokes equations:

- ✓ Moment of Fluid interface representation [1]
- ✓ Adaptive Mesh Refinement (AMReX)
- ✓ Large Eddy Simulation (WALE)
- ✓ Fully compressible formulation [2]
- ✓ Non-conformal moving wall boundaries [3,4]
- ✓ Cavitation [5]
- ✓ Evaporation and boiling [6,7]

[1] M. Jemison, et al., *J. Sci. Comput.* 54(2-3) (2013) 454-491.

[2] M. Jemison, M. Sussman, M. Arienti, *J. Comput. Phys.*, 279, (2014) 182-217.

[3] M. Arienti and M. Sussman, *Int. J. of Multiphase Flow* 59: 1-14 (2014).

[4] M. Arienti and M. Sussman, *Int. J. of Multiphase Flow* 88, 205-221 (2017).

[5] M. Arienti, E. Wenzel, B.A. Sforzo, C.F. Powell, *Proceedings of the Combustion Institute* (2020).

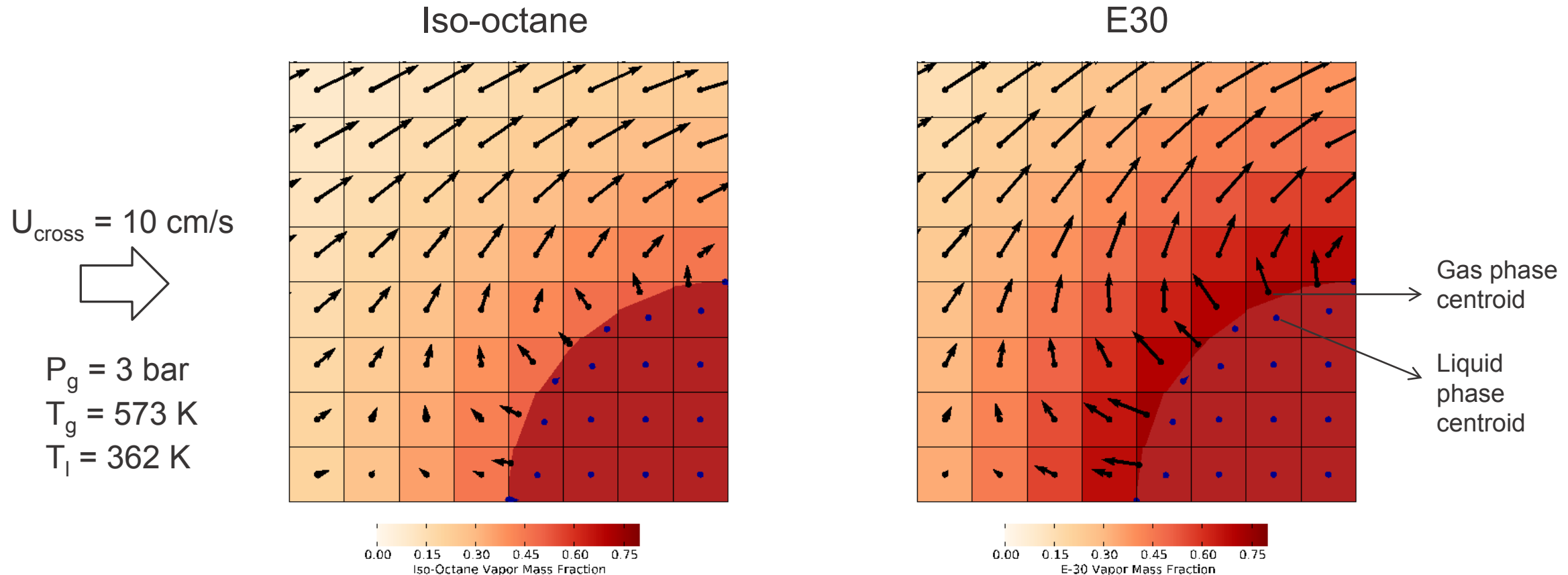
[6] E. Wenzel and M. Arienti, *ILASS-Americas* (2021).

[7] E. Wenzel and M. Arienti, “A conservative framework for the modeling and simulation of evaporation in compressible flow systems” – submitted to *JCP*.

Droplet in crossflow example: relevance of Stefan flow



- E30 has lower vapor pressure, generally leading to larger evaporation rate
- High rates of evaporation provide insulating layer of cool gas and thicken boundary layers
- In turn, the phase change rate depends on the boundary layer thickness



Computational challenge

- Problem: phase change introduces velocity discontinuity at the interface
 - Directly applying the divergence operator would impose an unphysically large momentum increment
- Solution:
 - Introduce cell-centered, phase-specific velocity

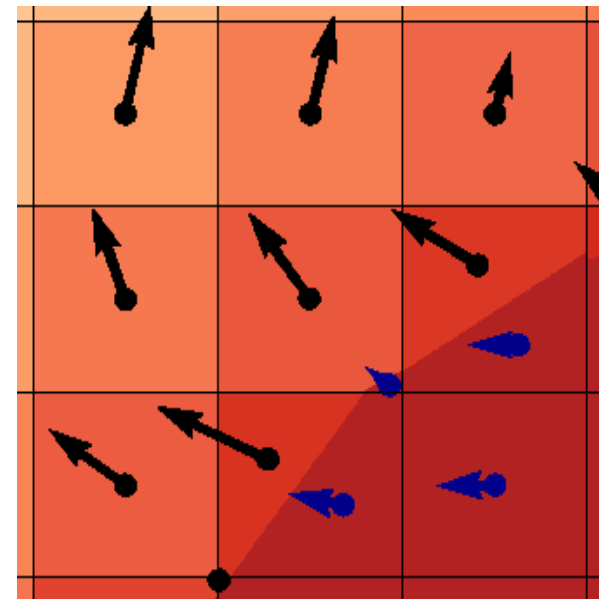
$$u_{g,i}^{n+1} - u_{l,i}^{n+1} = \dot{m}_i^d \left(\frac{1}{\rho_{g,i}^a} - \frac{1}{\rho_{l,i}^a} \right) n_x^d$$

$$\phi_{g,i}^{n+1} \rho_{g,i}^{n+1} u_{g,i}^{n+1} + \phi_{l,i}^{n+1} \rho_{l,i}^{n+1} u_{l,i}^{n+1} = \rho_i^{n+1} u_i^{n+1}$$

- Introduce face-centered, phase specific velocity

$$u_{g,i+1/2}^{n+1} = \frac{\sum_j u_{g,j}^{n+1} W_{ij}}{\sum_j W_{ij}} \quad u_{l,i+1/2}^{n+1} = \frac{\sum_j u_{l,j}^{n+1} W_{ij}}{\sum_j W_{ij}}$$

Velocity field diagram



$$u_{l,i}$$

$$u_{g,i}$$

$$u_{l,i+1/2}$$

$$u_{g,i+1/2}$$

$$u_{i+1/2}$$

Computational challenge



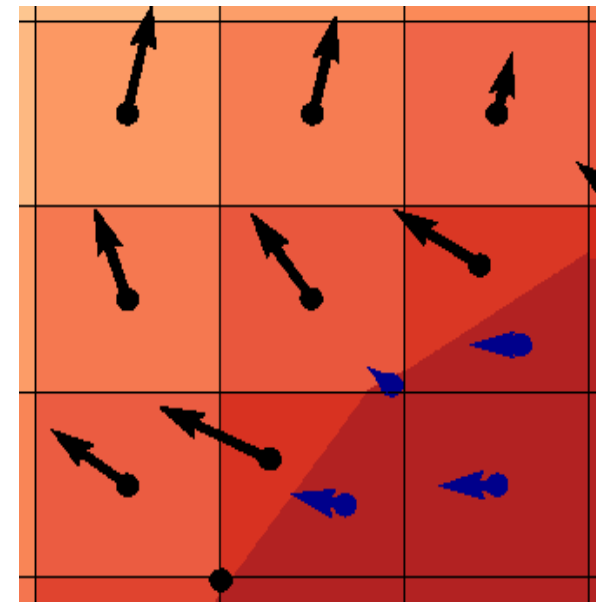
- Problem: phase change introduces velocity discontinuity at the interface
 - Directly applying the divergence operator would impose an unphysically large momentum increment
- Solution:
 - Solve augmented single-fluid pressure equation
 - Conservatively extract phase-specific velocities from single-fluid velocities

$$\phi_{g,i}^{n+1} \rho_{g,i}^{n+1} u_{g,i}^{n+1} + \phi_{l,i}^{n+1} \rho_{l,i}^{n+1} u_{l,i}^{n+1} = \rho_i^{n+1} u_i^{n+1}$$

$$u_{g,i}^{n+1} - u_{l,i}^{n+1} = \dot{m}_i^d \left(\frac{1}{\rho_{g,i}^a} - \frac{1}{\rho_{l,i}^a} \right) n_x^d$$

- Transport all conservative quantities with phase-specific velocities; transport MOF quantities with liquid-phase velocity; apply consistency constraints

Velocity field diagram



$$u_{l,i}$$

$$u_{g,i}$$

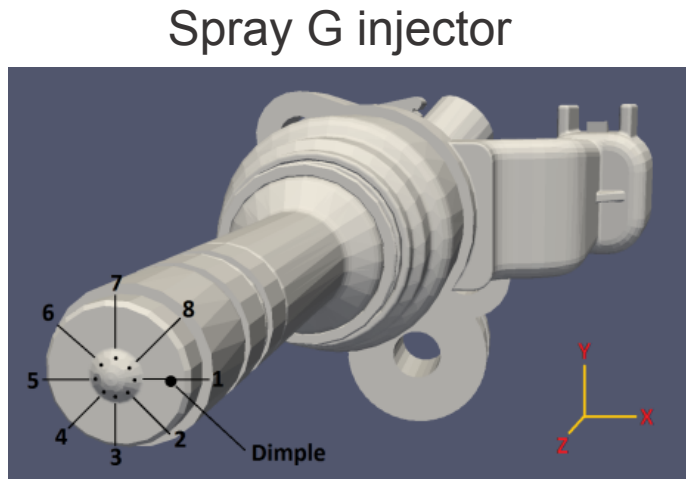
$$u_{l,i+1/2}$$

$$u_{g,i+1/2}$$

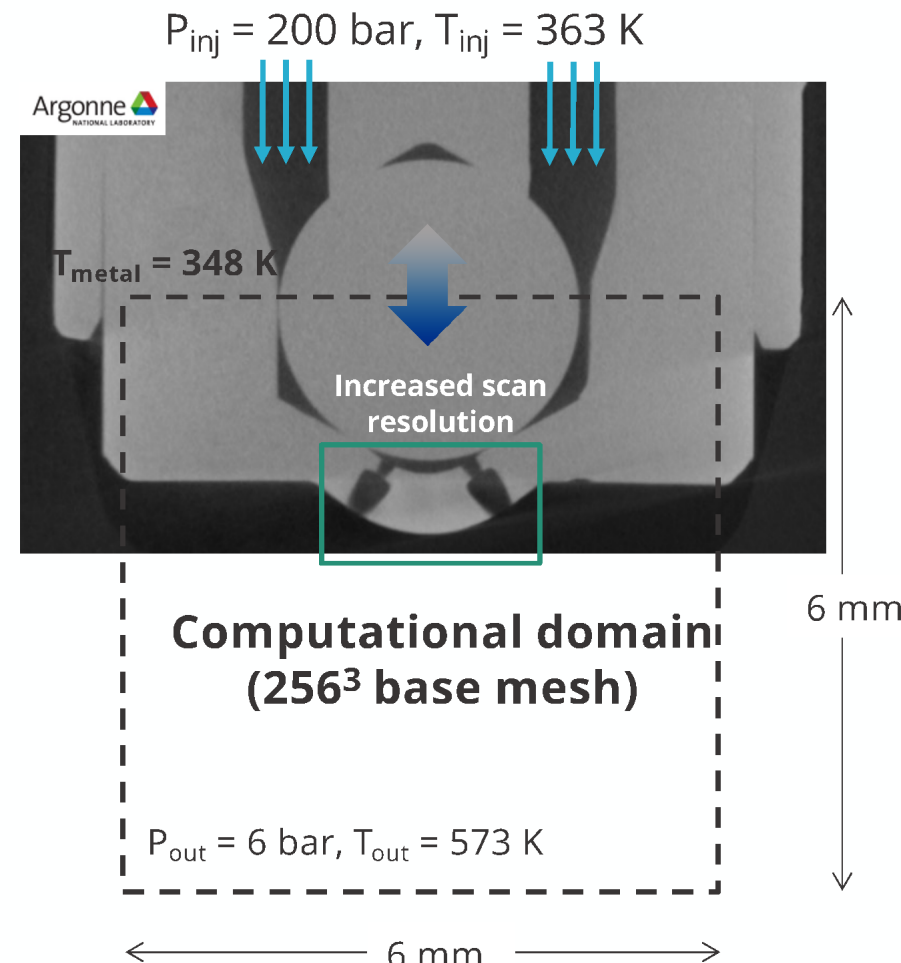
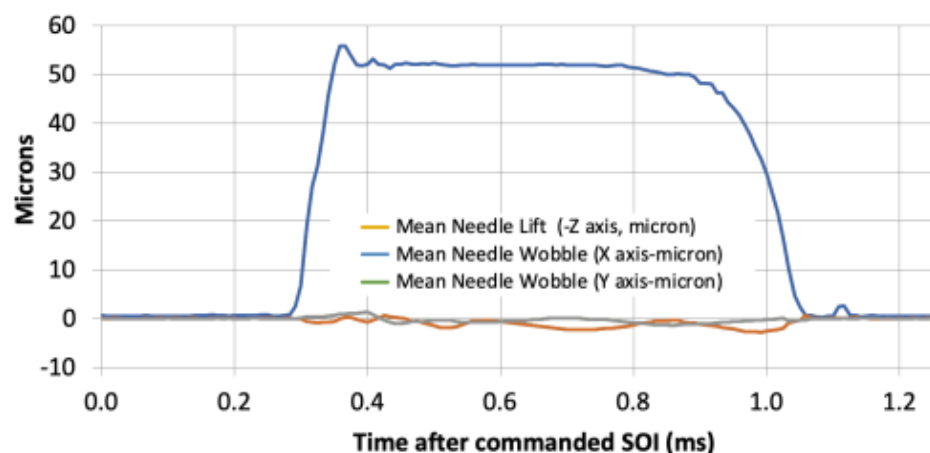
$$u_{i+1/2}$$

Fully open vs. closing pintle and near-injector phase change

- ECN G1 with up to 450million cells reaching $\Delta x_{\min} = 5.86 \mu\text{m}$ (2 levels of refinement)



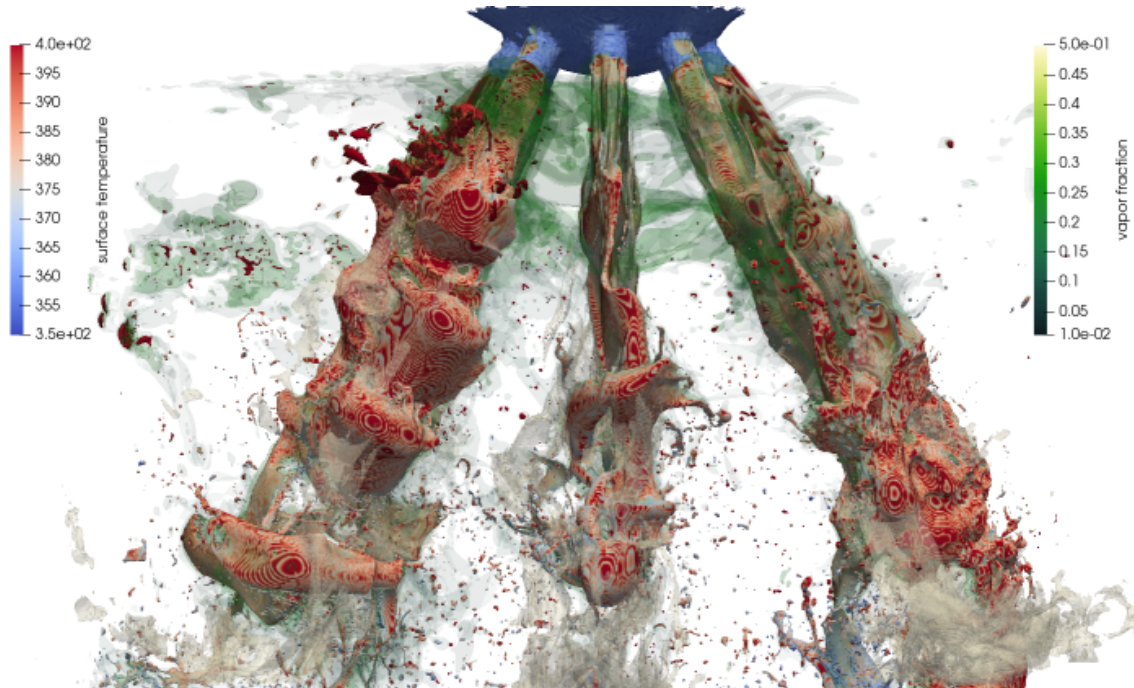
Lift and Wobble for ECN Spray G #28



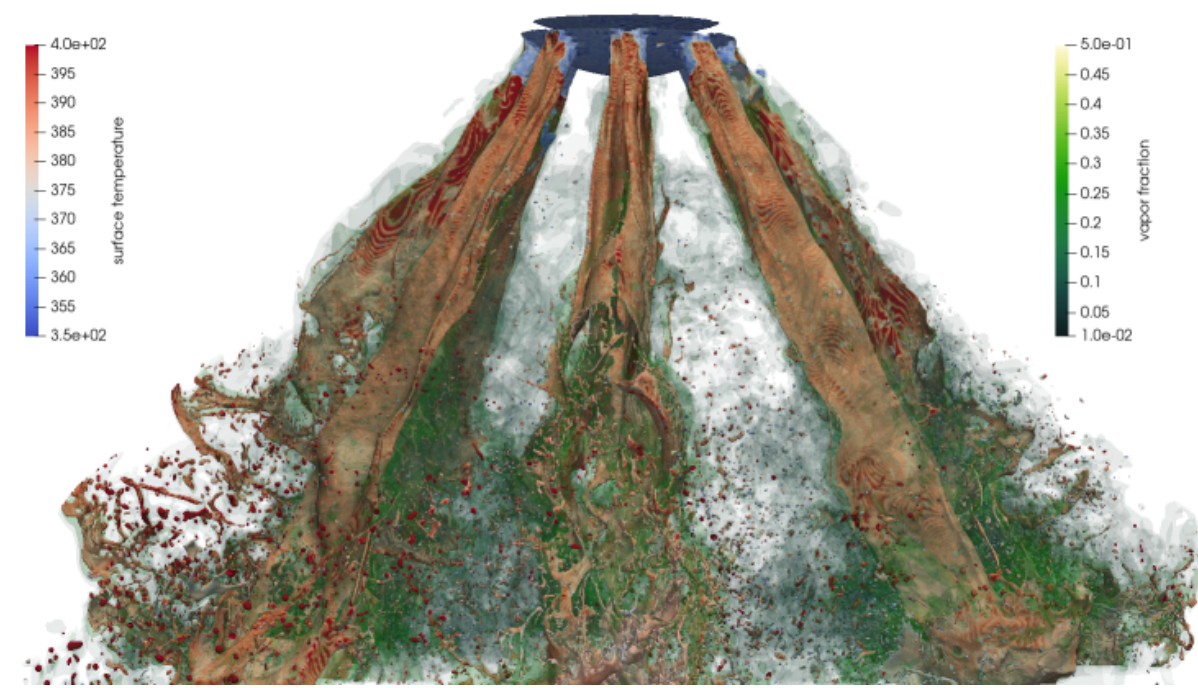
Comparison snapshots with fully open pintle

Observed difference in spray angle and jet structure, with enhanced vaporization for E30

Iso-octane



E30

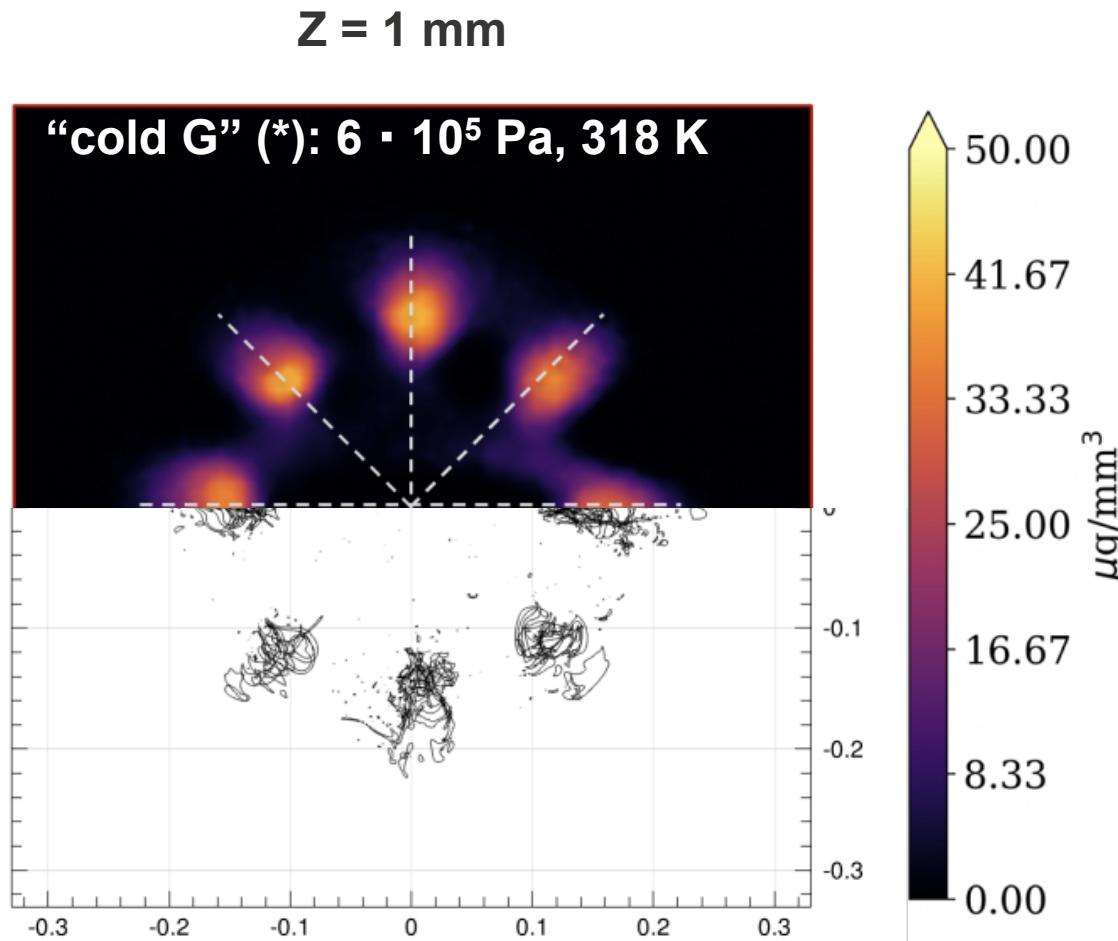


Images obtained by jointly imaging liquid surface (colored by T) and three iso-surfaces for $Y_{\text{vapor}} = 0.1, 0.25, 0.50$

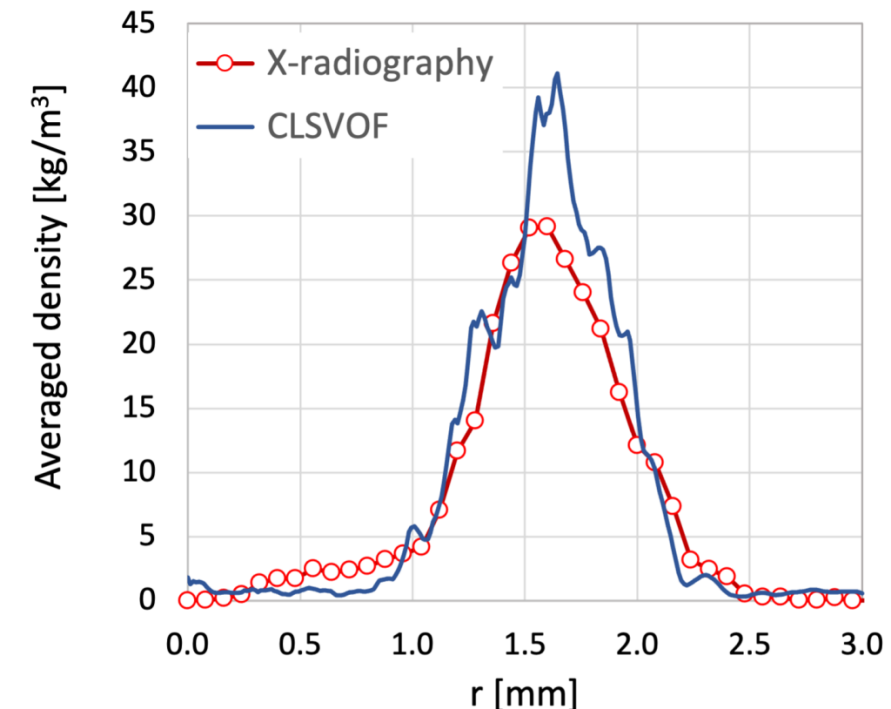
- regression rate: $v_s = \frac{\dot{m}_v}{A_v \rho_l} \sim 0.73 \text{ cm/s}$ $\sim 0.69 \text{ cm/s}$

Comparison with data: X-radiography from ANL

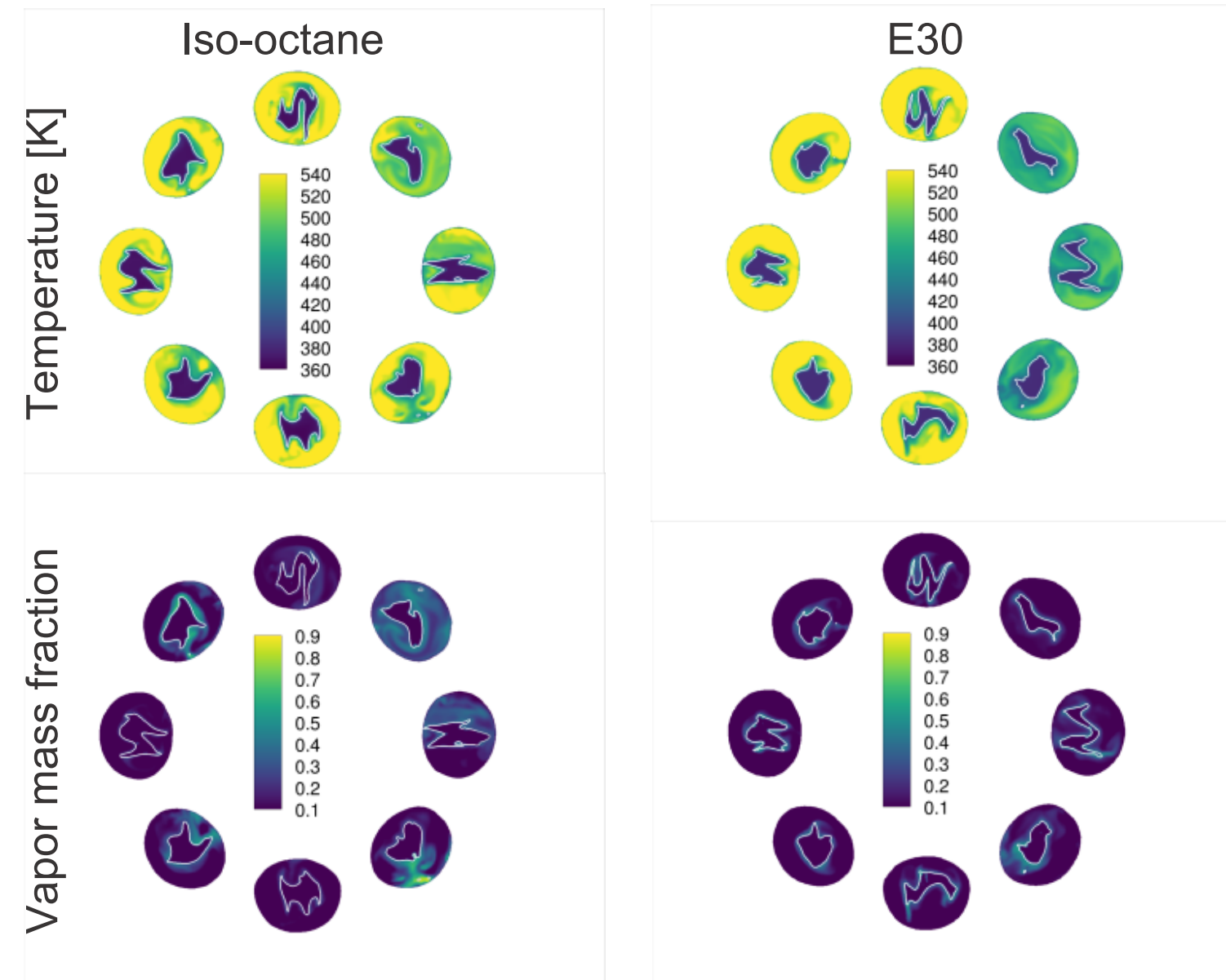
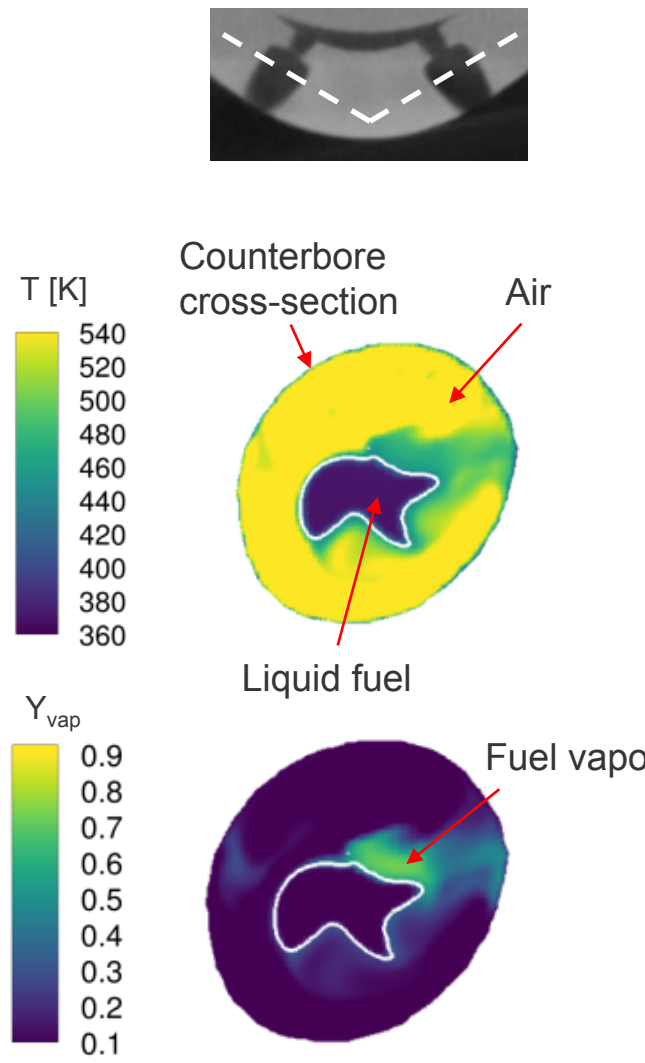
Relatively good agreement considering the shorter averaging time of the simulation



Average of the 8 density profiles passing through the nominal centers of the jets

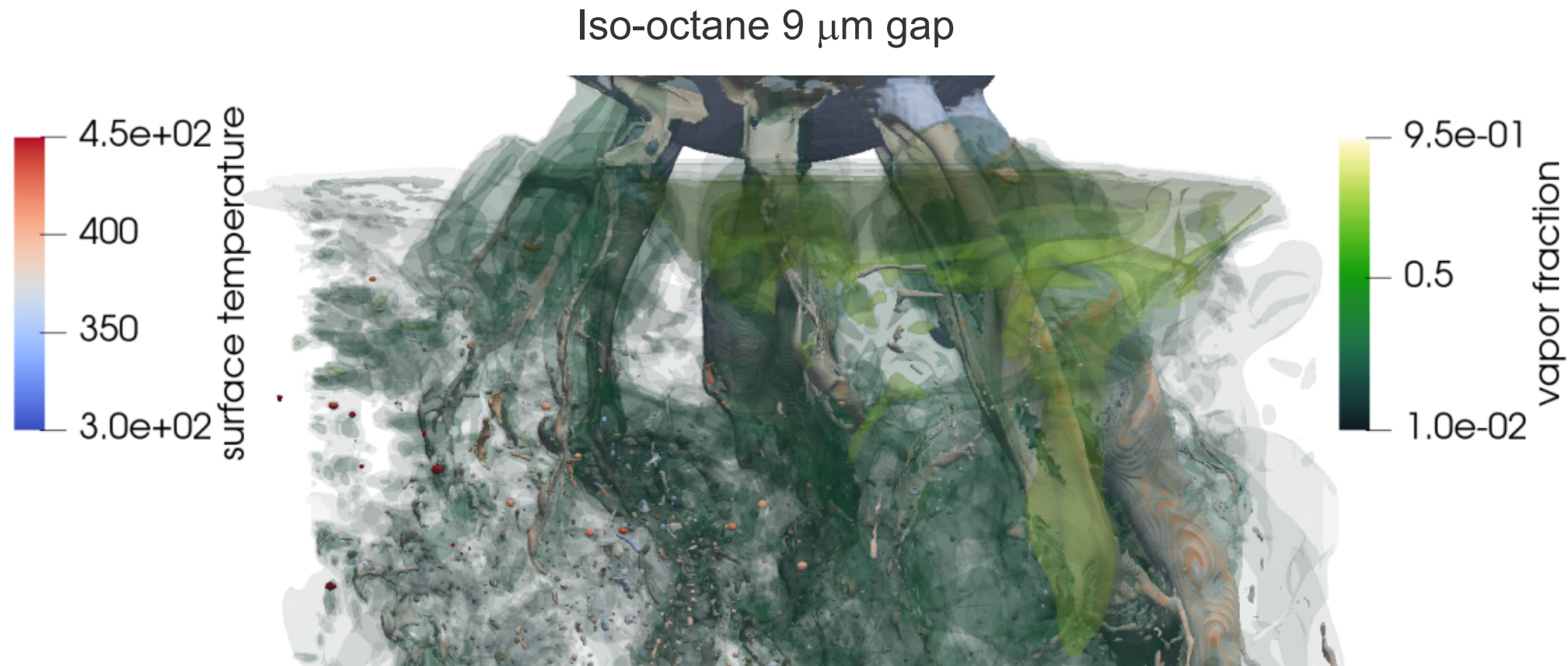


Flow passing through the counterbores at fully open conditions

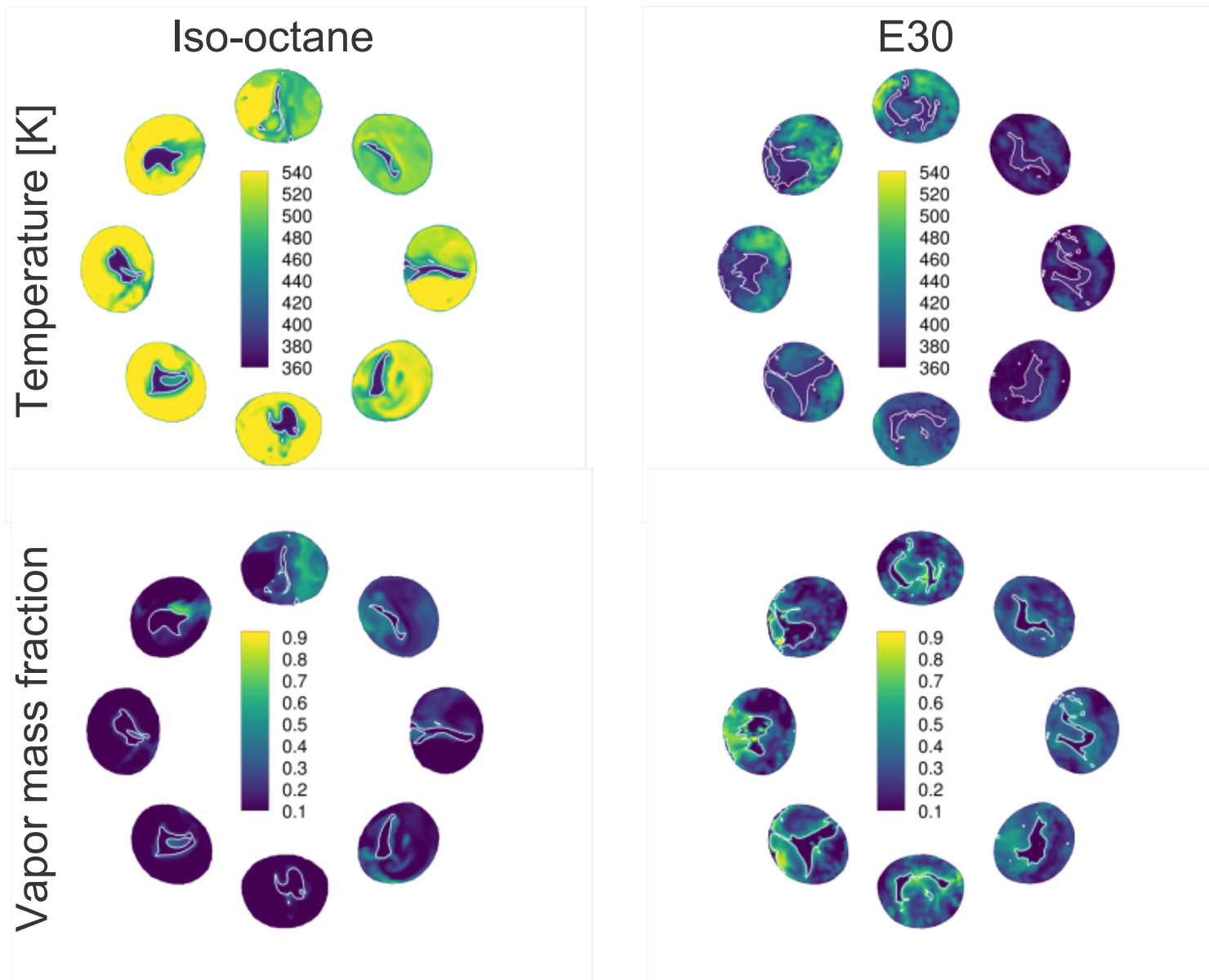


Toward end of injection for iso-octane

Increased amount of vapor – no evidence of boiling



Entrainment of hot gas is counterbalanced by cooling effect of E30



Conclusions



- A sharp-interface method for the multiphase Navier-Stokes equations is applied to calculate the vapor concentration in the counterbores of a gasoline injector
- $Pe \sim 3 \Rightarrow$ co-evaporation model – but it is only an average value for specific injection conditions
- Differences between neat iso-octane and E30 are particularly clear toward the end of injection
 - The simulation shows that gas stops being entrained in the counterbores during the closing transient;
 - It also shows that the temperature increase at the liquid surface is mitigated by the cooling effect of evaporation only in the case of E30
- Work is in progress to analyze the CFD results and provide further insight into the primary atomization processes



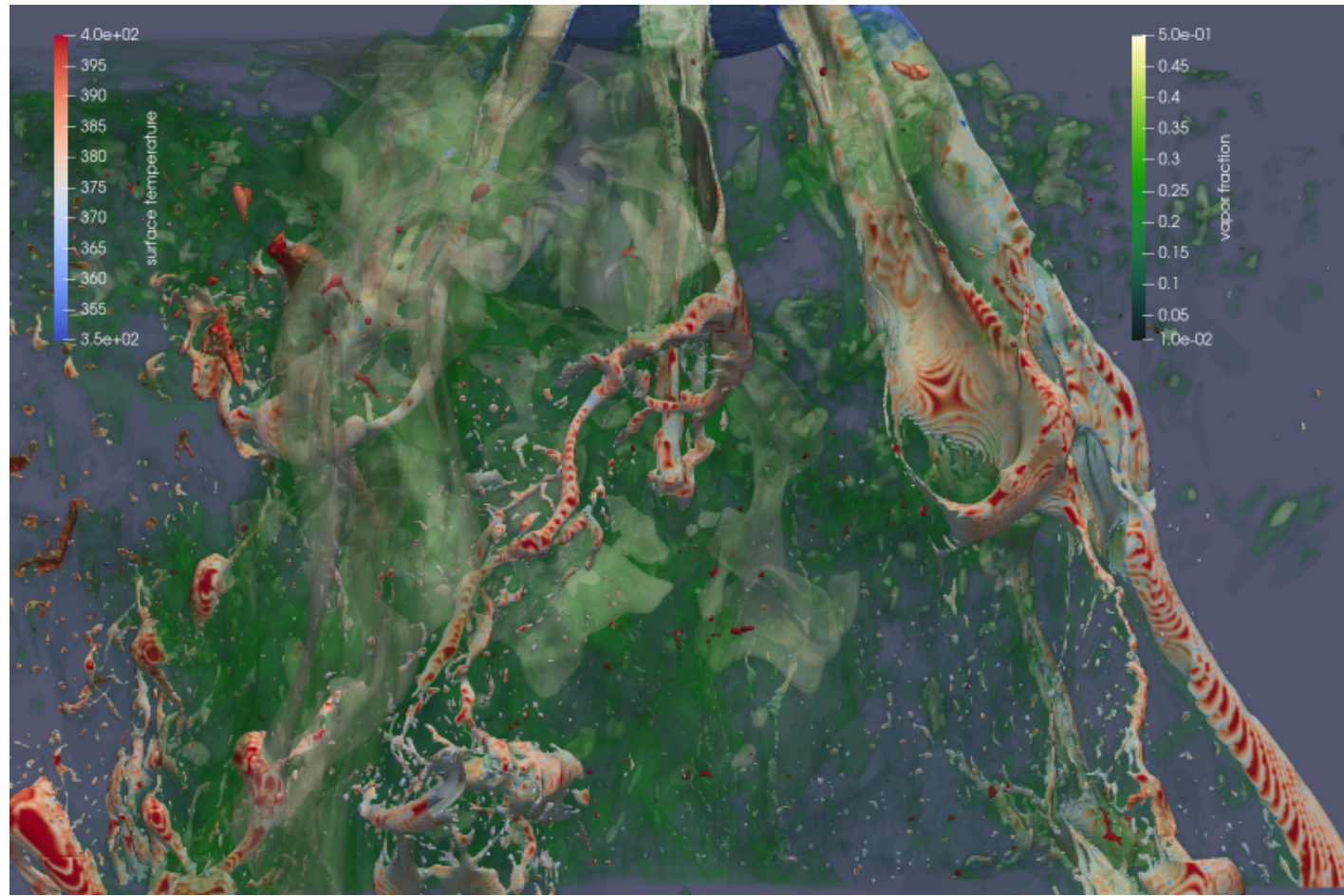
THANK YOU

Questions?

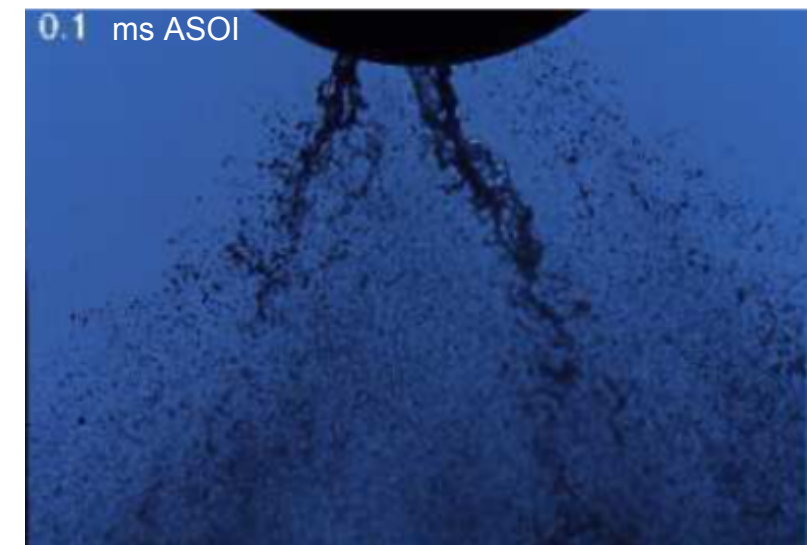
Close-up showing evidence of dribbling at end of injection



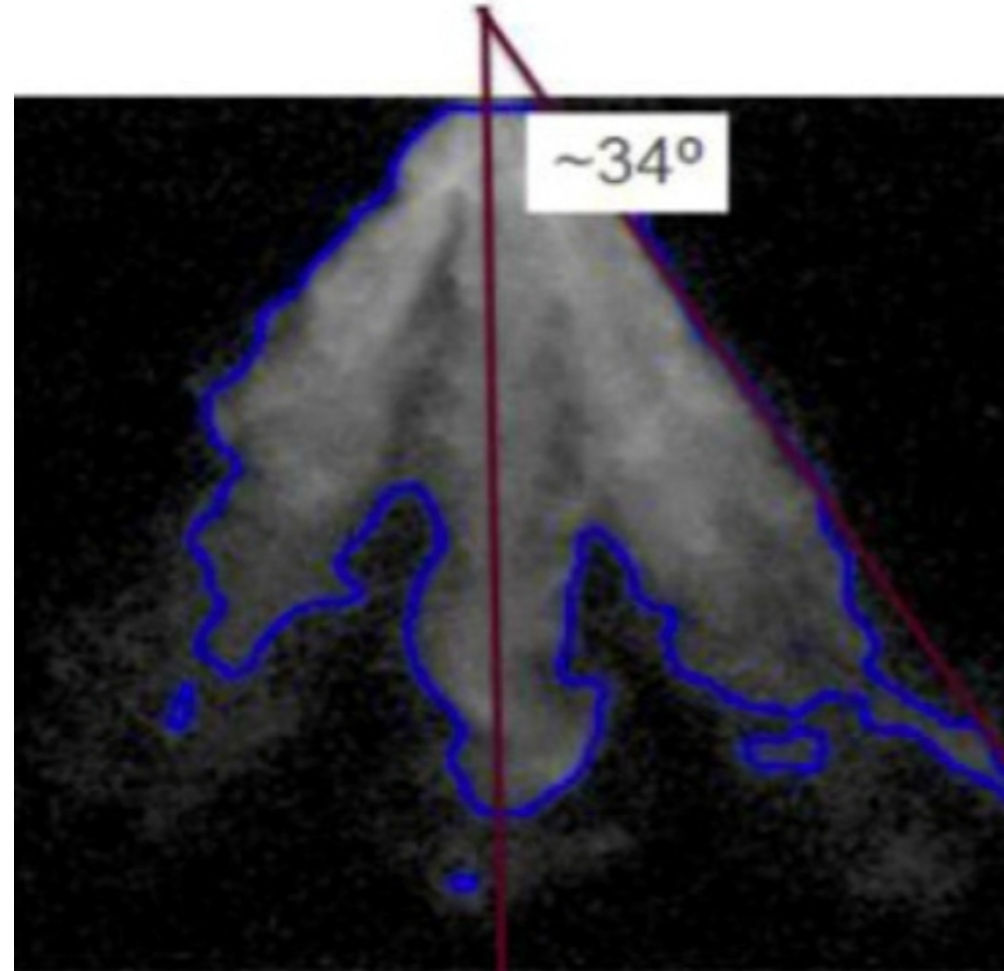
Iso-octane 9 μm gap



commercial gasoline with 5% ethanol



Six-hole injector at ambient conditions
Hélie, et al., International Journal of
Engine Research 22.1 (2021): 125-139.



Numerical discretization of evaporating fuel sprays

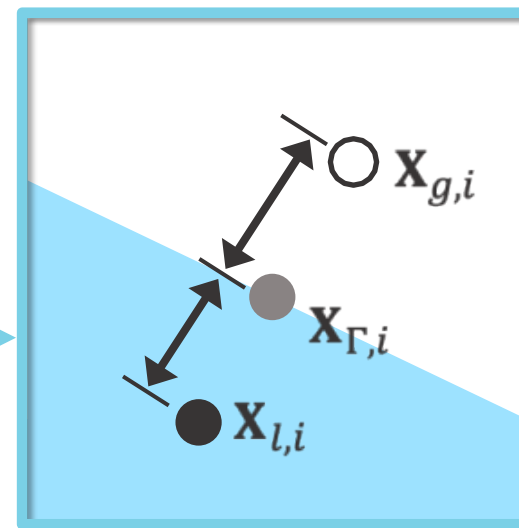


- Sharp-interface discretization (no Lagrangian droplets or associated models)
- Liquid and gas treated as compressible
- Conserved quantities stored at liquid/gas center of mass in each computational cell
- Diffusion and phase change defined by a novel, operator-split methodology that is consistent and conservative

Windowed view of full-scale spray simulation



Interface reconstruction in computational cell i

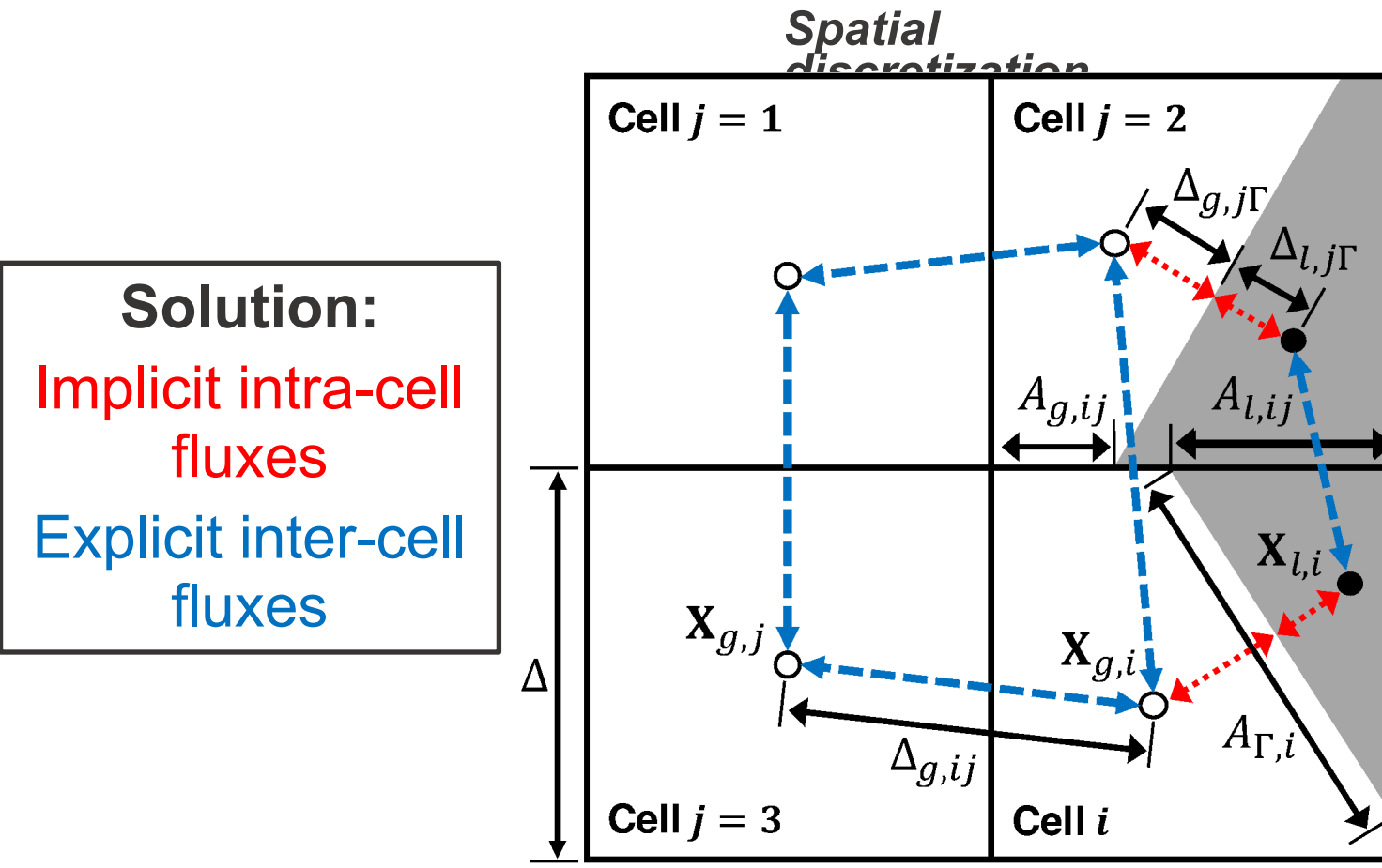


Navier-Stokes
equations solved at
Liquid/Gas centers-of-
mass $\mathbf{X}_{l,i}$ and $\mathbf{X}_{g,i}$

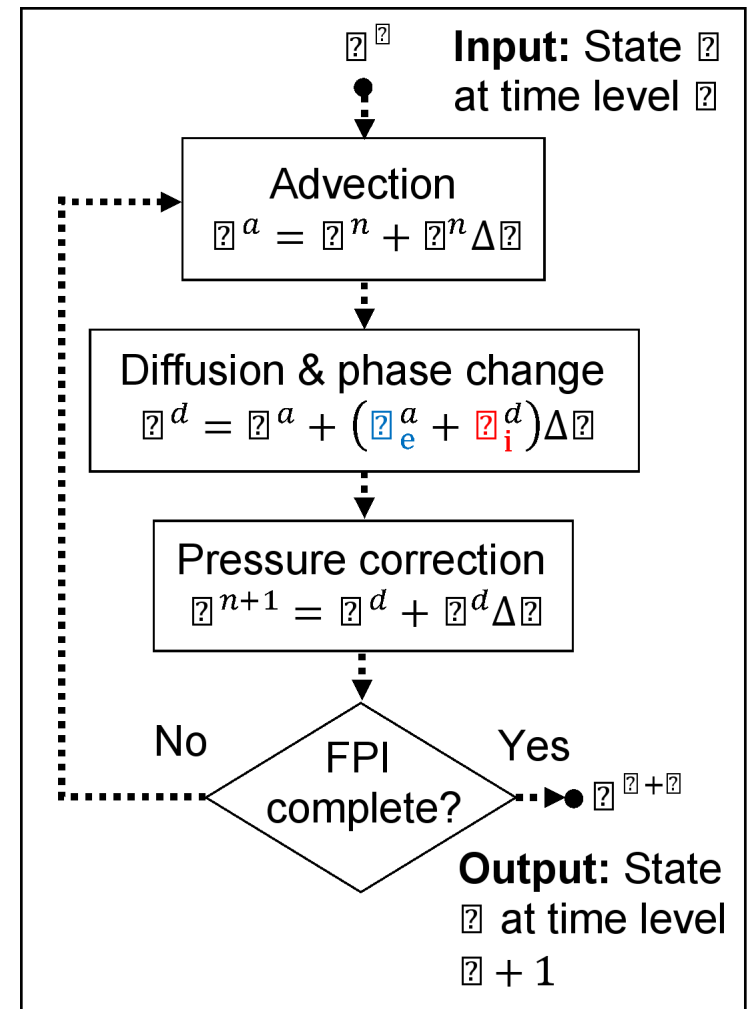
Interfacial quantities
required at $\mathbf{X}_{\Gamma,i}$ to
quantify heat/mass
transfer

Operator-split, mixed-time level integration approach

- Sharp interfaces require implicit time integration
- Capillary dynamics require small time steps
- Phase change systems are tightly-coupled



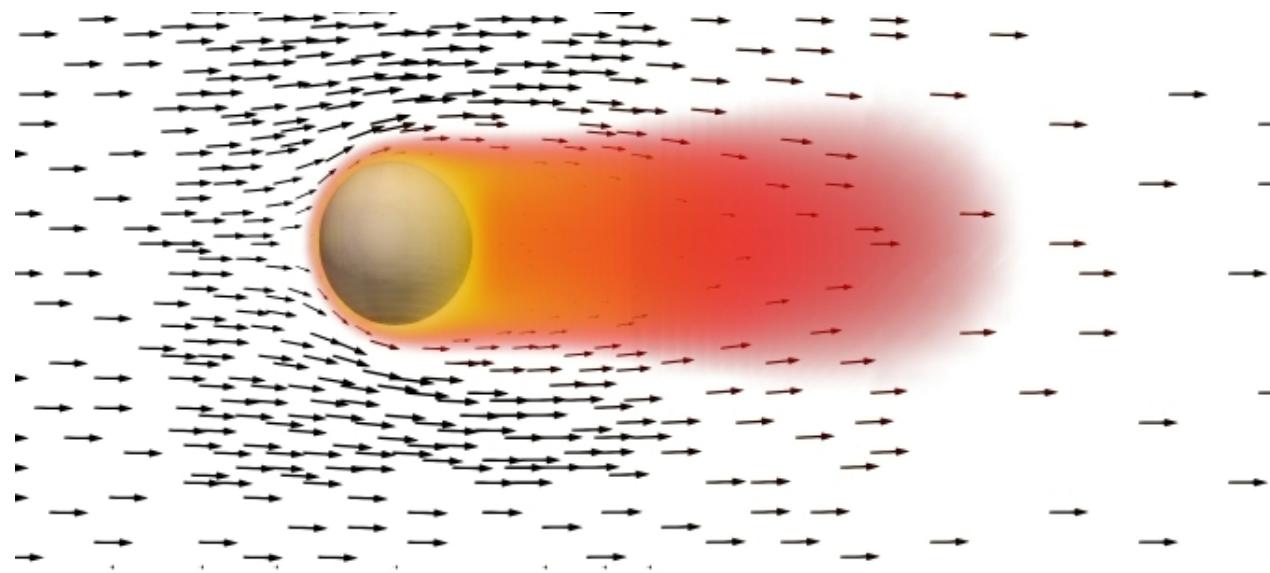
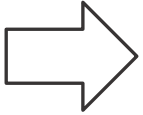
Temporal discretization



200 μm diameter iso-octane droplets evaporating



$U_{\text{cross}} = 500 \text{ cm/s}$



$P_g = 3 \text{ bar}$
 $T_g = 573 \text{ K}$
 $T_l = 362 \text{ K}$

$U_{\text{cross}} = 62.5 \text{ cm/s}$

